Experimental Investigation on Aerodynamic Control of a Wing with Distributed Plasma Actuators*

HAN Menghu (韩孟虎)[1], LI Jun (李军)[1], LIANG Hua (梁华)[1],
NIU Zhongguo (牛中国)[2], ZHAO Guangyin (赵光银)[1]

[1]Science and Technology on Plasma Dynamics Laboratory, Air Force Engineering University, Xi'an 710038, China
[2]Aviation Industry Corporation of China, Harbin 150001, China

Abstract Experimental investigation of active flow control on the aerodynamic performance of a flying wing is conducted. Subsonic wind tunnel tests are performed using a model of a 35° swept flying wing with an nanosecond dielectric barrier discharge (NS-DBD) plasma actuator, which is installed symmetrically on the wing leading edge. The lift and drag coefficient, lift-to-drag ratio and pitching moment coefficient are tested by a six-component force balance for a range of angles of attack. The results indicate that a 44.5% increase in the lift coefficient, a 34.2% decrease in the drag coefficient and a 22.4% increase in the maximum lift-to-drag ratio can be achieved as compared with the baseline case. The effects of several actuation parameters are also investigated, and the results show that control efficiency demonstrates a strong dependence on actuation location and frequency. Furthermore, we highlight the use of distributed plasma actuators at the leading edge to enhance the aerodynamic performance, giving insight into the different mechanism of separation control and vortex control, which shows tremendous potential in practical flow control for a broad range of angles of attack.

Keywords: plasma, flow separation control, NS-DBD, flying wing sequence

PACS: *47.85.Gj*

DOI: 10.1088/1009-0630/17/6/11

(Some figures may appear in colour only in the online journal)

1 Introduction

In recent years, the flying wing has drawn the attention of many researchers for its promising prospect in military and commercial use. It shows some tremendous advantages, including its low weight, large wing area, low drag and excellent stealth character. Many different configurations of the flying-wing-type unmanned combat aerial vehicle (UCAV) have been investigated in wind tunnels. However, there are also some challenging problems for the flying wing [1,2], such as the low maximum lift coefficient, the low degree of static instability in the longitudinal channel and the low efficiency of the high-lift devices at high angles of attack.

In order to improve the aerodynamic performance of aircrafts, many innovative flow-control actuators and techniques have been developed over recent years [3,4]. Among them, the dielectric barrier discharge (DBD) plasma actuator offers tremendous potential as an active flow-control device due to it having no moving parts, a resurface adapting ability, low power requirement, and a fast time response. It has been proved to be an efficient approach of aerodynamic control in many situations [5−9]. The dominant mechanism of this kind of DBD actuator is the time-averaged body force which can produce acceleration in the boundary layer. Furthermore, recent advances in plasma control have demonstrated that nanosecond pulsed DBD plasma is more effective than Alternating Current dielectric barrier discharge (AC DBD) plasma [10−12]. Experiments have indicated that the NS-DBD plasma actuator can successfully control separation when used on the leading edge, especially at high speed [13].

The application of plasma actuation to control aerodynamic coefficients of swept wings or flying wings has been widely studied. Greenblatt et al. [14,15] considered the control of a leading edge vortex on a 60° swept semispan delta wing by means of AC DBD plasma actuators at speeds below 10 m/s, and maximum lift enhancements were observed at pulsed reduced frequency F^+=1. The flow field was also investigated by means of flow visualization, and the PIV results indicated that the major contribution to lift enhancement occurred near the wing apex and the vortex above the wing traversed an almost circular path with plasma control. Anatoly Maslov et al. [16] investigated the separation control on a model of a swept wing by means of an AC DBD plasma actuator at low speed. Surface pressure measurements and flow visualization indicated that global separation could be mitigated with control. Also, the control efficiency demonstrated a strong de-

*supported by National Natural Science Foundation of China (Nos. 51276197, 51207169 and 51336011)

pendence on the duty cycle and frequency of the discharge. Alexey et al. [17] also studied the possibility of vortex flow control on a 65° swept delta-wing by means of AC DBD plasma actuators at subsonic speed, the flow visualization indicated that the plasma actuator could influence the vortex breakdown position and lead to vortex stabilization when operating at burst mode. The highest efficiency was achieved with the DBD actuator placed at the leading edge across the vortex flow.

From a practical point of view, the future technology for aerodynamic control of an aircraft is by using active flow control in a distributed manner, as required by different missions. The plasma actuator matches the condition due to its resurface adapting ability. Mehul and Patel et al. [18] investigated the use of distributed AC DBD plasma actuators at the leading and trailing edges of a 1303 unmanned aerial vehicle (UAV) to provide aerodynamic control; the results showed that plasma actuators could provide aerodynamic control over a broad range of angles of attack. Nelson and Corke et al. [19] studied the distributed plasma actuators for improving performance on a smart wind turbine blade, for the purpose of controlling different parts of the turbine blade. The results showed that both the leading and the trailing edge control could enhance the lift coefficients.

Compared to the conventional control with AC DBD plasma actuators, a new application of leading edge NS-DBD plasma actuation to realize aerodynamic control on a flying wing model with a 35° swept angle is investigated at subsonic flow speed. Lift and drag coefficients, the lift-to-drag ratio and the pitching moment coefficient are measured by a six-component balance for an angle of attack up to 30°. The effects of actuator frequency and location are also investigated to estimate the control efficiency on aerodynamic performance. Furthermore, the present work also highlights the use of distributed plasma actuators to enhance the aerodynamic performance by mounting several actuator configurations at the leading edge of the wing.

2 Experimental setup

2.1 Wind tunnel

The experiments were conducted in the FL-5 low-speed wind tunnel at the Aerodynamics Research Institute. The facility is an open-return wind tunnel with a 1.95 m long test section and a circular cross section of 1.5 m diameter. The maximum air speed in the wind tunnel is 53 m/s, and the turbulence intensity is below 1%. The photo of the test section of the wind tunnel is shown in Fig. 1(a).

2.2 Wind model and plasma actuators

The wind tunnel model used in the present study is a typical flying wing with a 35° sweep angle at the leading and trailing edges, with a varying cross-section along the wing span. The shape of the leading edge along the wing span is a little sharp at the front and the aft, whereas the shape of the leading edge at the middle wing span is a little blunt. The total wing span is approximately 0.953 m and the fuselage length is about 0.386 m. The photo of the model with the plasma actuator mounted symmetrically on the wing's leading edge is shown in Fig. 1(b).

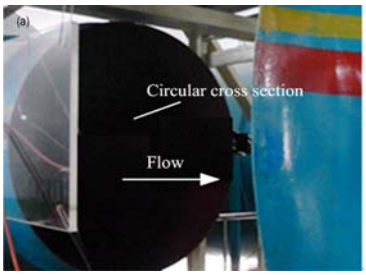

(a) The test section of the wind tunnel

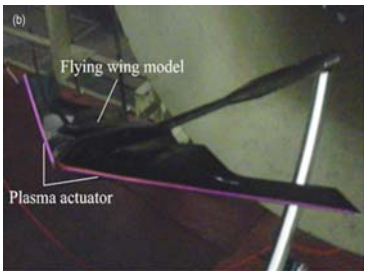

(b) The flying wing model with plasma

Fig.1 Test section of the wind tunnel with a flying wing model

The DBD plasma actuator consists of two electrodes and a dielectric layer. The exposed electrode is 3 mm in width, and the covered one is 5 mm in width. They overlap by a very small amount, which can generate uniform plasma along the leading edge. The dielectric layer is made of three layers of Kapton tape and is 0.2 mm in depth.

In the present study, tests are performed to evaluate the effects of pulsed location on aerodynamic performance enhancement. Based on lots of previous studies, a plasma actuator is located on three locations of the wing's leading edge. The actuation position, which is between the two electrodes, is placed at 0 mm, 3 mm and 10 mm from the leading edge, named as type C, A and B, respectively. The schematic illustration of the plasma actuator is shown in Fig. 2.

With distributed plasma control, three different actuator arrangements of type A are investigated at the leading edge, which is shown in Fig. 3. The tested wing is divided into three parts: inner wing I, inner wing II and outer wing.

2.3 Measurements

The aerodynamic force and moment coefficients of the model are measured by a six-component force balance for angles of attack up to 30°. The overall absolute uncertainty in the lift and drag coefficients are less than 0.005 and 0.001, respectively, based on repeated force measurement on the calibration model. The experiments are performed with free-stream velocity of

30 m/s, corresponding to the chord Reynolds number of 4.6×10^5.

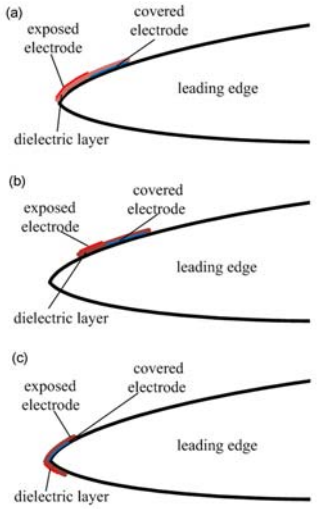

(a) Plasma actuator of type A, (b) Plasma actuator of type B, (c) Plasma actuator of type C

Fig.2 Three types of plasma actuator mounted on the wing's leading edge

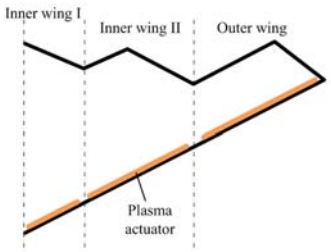

Fig.3 The flying wing model with distributed plasma actuators

A high voltage generator was used to generate plasma between the two electrodes of the actuator. The output voltage and the frequency could be varied in the ranges of 0-80 kV and 0.2-2 kHz, respectively. The discharge voltage and current were measured by four-channel Tektronix DPO4104 oscilloscopes, a Tektronix P6015A high voltage probe, a Tektronix TCP312 and TCPA300 current probe. The measurements of pulsed voltage and current are shown in Fig. 4. Previous experiments have indicated that the pulsed amplitude of 12 kV results in satisfactory control. So, in the present control experiment, the actual pulsed amplitude is fixed at 12 kV, and the pulsed frequency ranges from 0.2 kHz to 1.2 kHz.

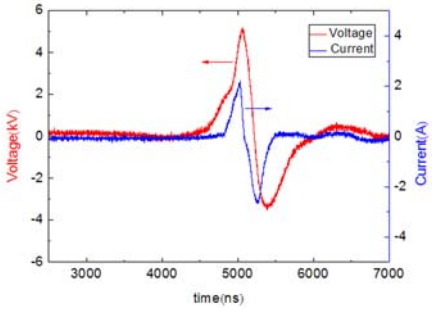

Fig.4 Measurements of pulsed voltage and current

3 Results and analysis

3.1 Results of actuation of different types

3.1.1 Results of type A actuation

Fig. 5 shows the results from the plasma actuator turned on and off for a free-stream velocity of 30 m/s. In the baseline case, the lift coefficient increases with an increase of the angle of attack, reaches a maximum value at $\alpha = 18^o$, and then decreases due to severe separation. The drag coefficient also increases as the angle of attack increases. But for α >18°, the drag coefficient increases more significantly, which may be caused by the separation on the upper surface of the wing.

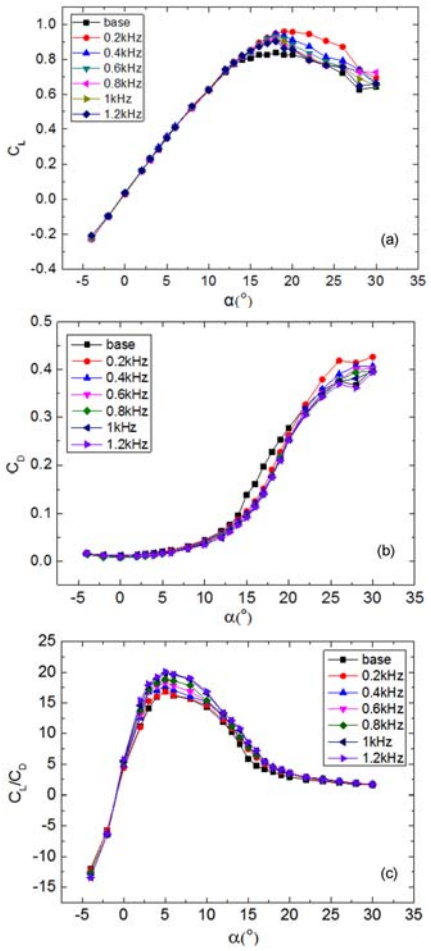

(a) Lift coefficient, (b) Drag coefficient, (c) Lift-to-drag ration

Fig.5 Results of type A actuation

Fig. 5(a) shows the detailed effect of pulsed frequency on the lift coefficient for frequencies ranging from 0.2 kHz to 1.2 kHz. The results indicate that control efficiency demonstrates a strong dependence on pulsed frequency. The lift enhancement increases with decreasing pulsed frequency, especially for stall angles of attack.

Fig. 5(b) illustrates a surprising decrease in the drag coefficient with plasma actuation. More decrease in the drag coefficient can be achieved with increasing pulsed frequency, which shows an opposite trend to the

change in lift coefficient. Given the pulsed frequency of 0.2 kHz, the value of the drag coefficient is larger than the value of the baseline for $\alpha > 22^{o}$, which indicates adverse effects of low frequency on decreasing drag.

Fig. 5(c) indicates that the change of lift and drag coefficients synthetically results in an obvious increase in the lift-to-drag ratio for a broad range of angles of attack at actuation frequency $f > 0.8$ kHz. For the actuation frequency of 0.2 kHz, the increment in the lift-to-drag ratio can be obtained only for angles of attack ranging from 10^{o} to 22^{o}. In general, it can be concluded that the increase in the lift-to-drag ratio is mainly attributed to the decrease in the drag coefficient for low angles of attack.

So, it can be concluded that low actuation frequency results in more enhancement in the lift coefficient, whereas high actuation frequency results in more decrease in the drag coefficient. Based on these results and the life of the plasma actuator, the following tests are conducted for an actuation frequency of 0.2 kHz and 1 kHz.

3.1.2 Results of type B actuation

Fig. 6 illustrates the effects of plasma actuators of type B on the aerodynamic performance of the model. In Fig. 6(a), increments in the lift coefficient can be obtained for high angles of attack with plasma actuation, showing a similar trend to the results of type A actuation. Given the actuation frequency of 1 kHz, the lift coefficient is nearly the same as the baseline case, which indicates that the actuator of type B cannot efficiently improve the lift performance at high frequency. However, as shown in Fig. 6(b), an obvious decrease in the drag coefficient can be obtained at frequency 1 kHz, also showing a similar trend to type A. For pulsed frequency 0.2 kHz, the result indicates a negative effect on decreasing drag for $\alpha > 20^{o}$. Fig. 6(c) shows an obvious increase in the lift-to-drag ratio for a broad range of angles of attack at pulsed frequency 1 kHz, also showing a similar trend as type A.

3.1.3 Results of type C actuation

The effects of plasma actuators of type C on aerodynamic performance with plasma actuation are shown in Fig. 7. The result shows an obvious increase in the lift coefficient and a decrease in the drag coefficient at all tested frequencies, which indicates that an increase in the lift coefficient can be obtained when the plasma actuator is placed closer to the wing's leading edge. However, in Fig. 7(c), the result of the lift-to-drag ratio shows obvious differences from the other two types. A negative effect can be observed for low angles of attack at both of the pulsed frequencies. For angles of attack ranging from 10^{o} to 24^{o}, an increase in the lift-to-drag ratio can be achieved, which is attributed to the obvious increase in the lift coefficient and a decrease in the drag coefficient.

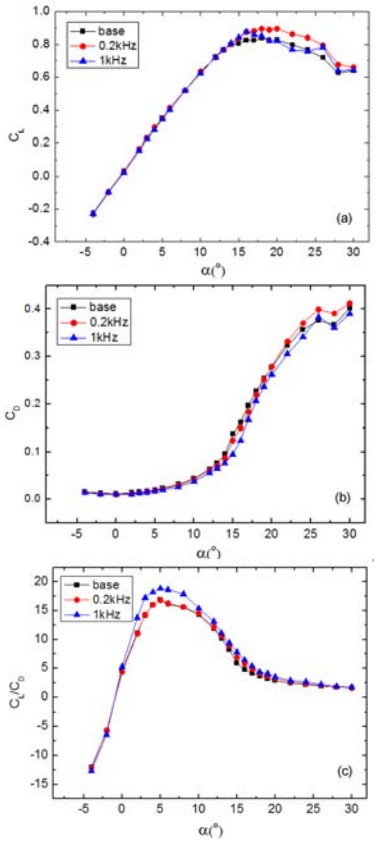

(a) Lift coefficient, (b) Drag coefficient, (c) Lift-to-drag ration

Fig.6 Results of type B actuation

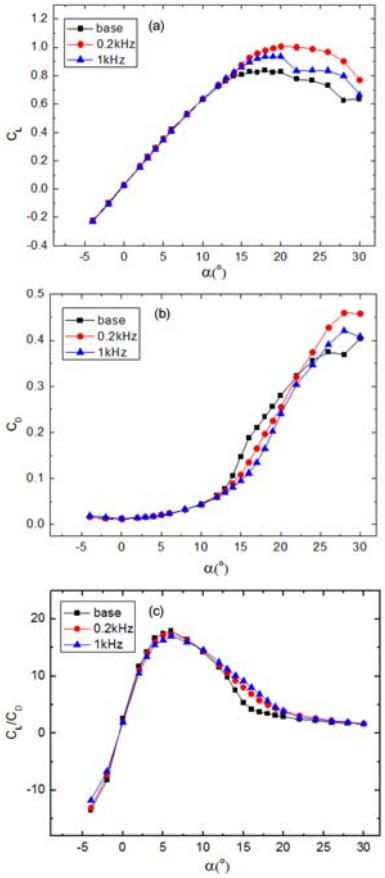

(a) Lift coefficient, (b) Drag coefficient, (c) Lift-to-drag ration

Fig.7 Effects of plasma actuator of type C actuation

3.1.4 Details between different actuation types

The detailed changes in aerodynamic performance for plasma actuators of different types are shown in Fig. 8. Obvious differences can be found in both lift and drag coefficients, which indicate that control efficiency demonstrates a strong dependence on the actuation location and frequency. As shown in Fig. 8(a), the values of δC_{L} , defined as $C_{\mathrm{L,control}} - C_{\mathrm{L,base}}$, all begin to increase from an angle of attack α =13°, reaching maximum values of 21.3%, 10.3% and 44.5% for type A, type B and type C actuation, respectively. Given the pulsed frequency of 1 kHz, Fig. 8(b) shows a slight negative effect on the lift coefficients at low angles of attack. However, for α >13°, an obvious lift enhancement also can be achieved for most angles of attack, but the value is lower than that at low frequency. So, the present results indicate that as the plasma actuation is closer to the leading edge of the flying wing and the actuation frequency is lower, more increment in lift performance can be obtained.

As shown in Fig. 8(c) and (d), there are also obvious differences in drag coefficient between plasma actuators of different types. For type A and type B actuation, decreases in drag coefficient can be obtained for α <20° at an actuation frequency of 0.2 kHz. However, for the type C one, the result shows a negative effect on the drag coefficient for α < 10°, and a decrease in the drag coefficient can be observed only for angles of attack ranging from 10° to 22°. Fig. 8(d) shows more decrease in drag coefficients when the actuation frequency is 1 kHz, and maximum values of 33.7%, 27.1% and 29.8% can be achieved for type A, type B and type C actuation, respectively.

Fig. 8(e) and (f) illustrate the change in the lift-to-drag ratio, which is defined as $C_{\mathrm{L}}/C_{\mathrm{D,control}} - C_{\mathrm{L}}/C_{\mathrm{D,base}}$ ($\delta C_{\mathrm{L}}/C_{\mathrm{D}}$). As can be seen, plasma actuation with high pulsed frequency causes enhancement for a large range of angles of attack, whereas a low pulsed frequency results in enhancement in the lift-to-drag ratio only for high angles of attack. For type A and type B plasma actuation, the value of $\delta C_{\mathrm{L}}/C_{\mathrm{D}}$ is higher than that of type C actuation for angles of attack α <13° and lower for larger angles of attack.

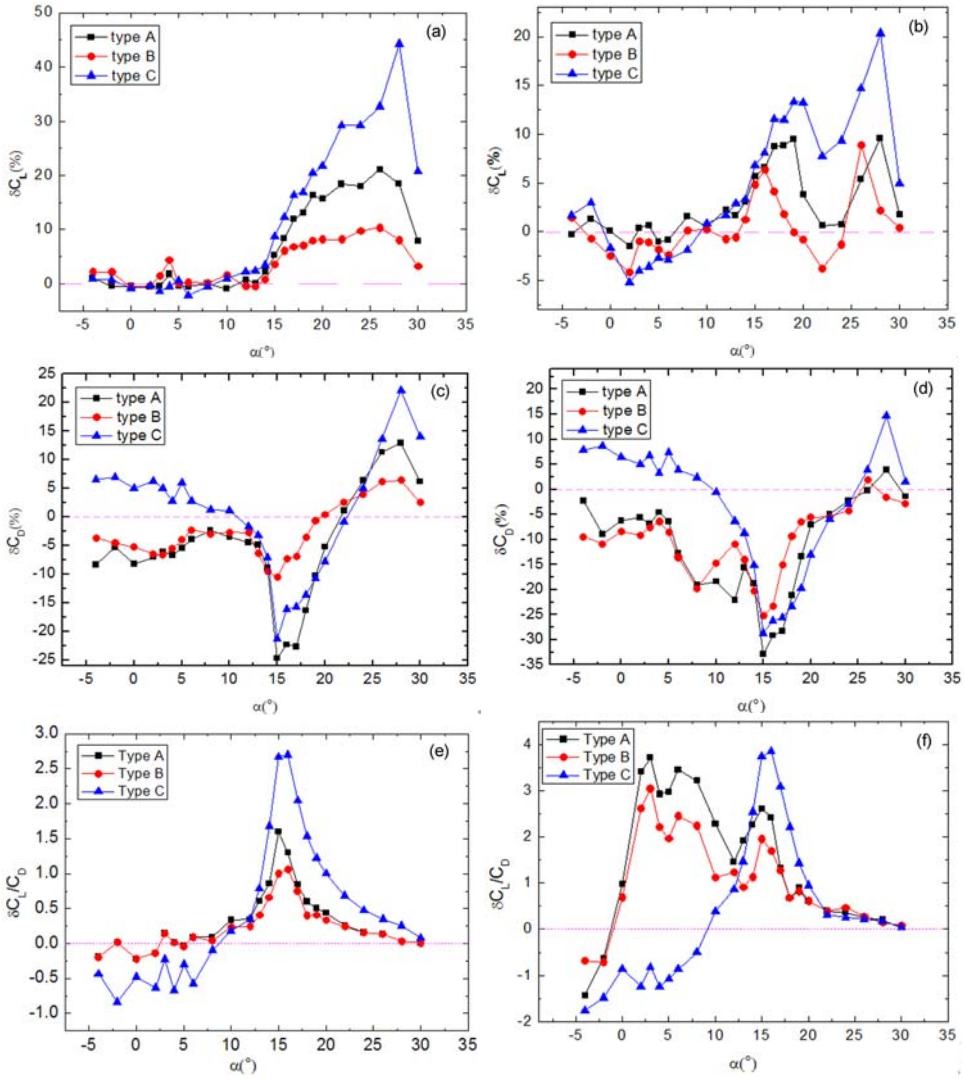

(a) The detailed change in C_{L}, 0.2 kHz, (b) The detailed change in C_{L}, 1 kHz, (c) The detailed change in C_{D}, 0.2 kHz, (d) The detailed change in C_{D}, 1 kHz, (e) The detailed change in $\delta C_{\mathrm{L}}/C_{\mathrm{D}}$, 0.2 kHz, (f) The detailed change in $\delta C_{\mathrm{L}}/C_{\mathrm{D}}$, 1 kHz

Fig.8 Detailed effects of plasma actuation on aerodynamic performance

3.1.5 Effects on pitching moment

For flying wings, the low degree of static stability in the longitudinal channel is still one of the challenging aerodynamic issues. So, experiments are conducted to determine the effects of a leading edge NS-DBD plasma actuator on the pitching moment coefficient of the wing model. Fig. 9 shows the results of plasma actuators of different types. The date also indicate that different changes in M_Z can be obtained by changing the pulsed location and frequency. For type A actuation, an obvious increase in M_Z for a high angle of attack can be obtained only at a pulsed frequency of 0.2 kHz. For the type B one, a negligible change in the pitching moment is produced for all tested frequencies. Fig. 9(c) shows that the obvious effect of the type C one on the pitching moment coefficient can be produced at high and low pulsed frequencies.

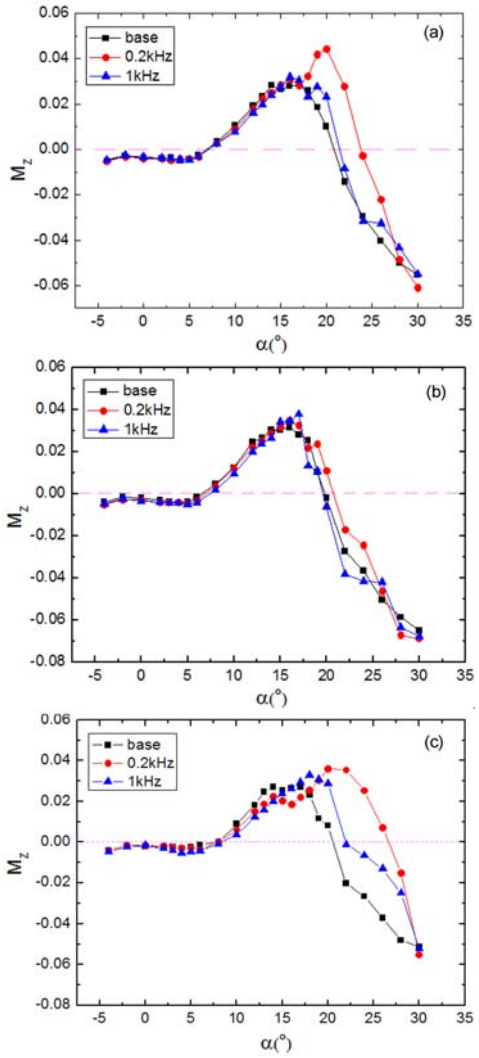

(a) Pitching moment coefficient, type A, (b) Pitching moment coefficient, type B, (c) Pitching moment coefficient, type C

Fig.9 Effects of pulsed frequency on pitching moment coefficients

The values of the pitching moment coefficient with plasma control are slightly lower than the baseline for α <18°, especially at high pulsed frequency. So, the test suggests that plasma actuation may be used for improving the static stability in the longitudinal channel.

3.2 Results of distributed plasma actuation

The results of applying plasma actuation in a distributed manner are shown in Fig. 10. The results indicate that the different actuation position has a huge effect on aerodynamic performance enhancement. The lift coefficient curves show that plasma actuation can produce controlled changes at high angles of attack, with some distinguishable differences between different actuation positions. Fig. 10(b) shows that inner wing II can provide the maximum contribution in lift enhancement. Drag coefficient can also be reduced at high angles of attack, and the trends with different actuation frequencies are the same. For the outer wing actuation, however, as shown in Fig. 10(f), reduction in the drag coefficient can be achieved at low angles of attack, resulting in an obvious change in the lift-to-drag ratio. So, we can conclude that the flow on the leeward surface of the outer wing is changed by plasma actuation, and that the reason may be related with the configuration of the wing and the flow around it. As the leading edge section of the wing is round and sharp for inner wing II and the outer wing, the flow around inner wing II is attached at low angles of attack, whereas the sharp and swept leading edge of the outer wing can lead to a vortex. Atkinson et al. [20] had studied the flow structure of a 1303 UAV configuration, which also had a varying cross-section leading edge. The oil flow is illustrated in Fig. 11. The plasma actuation has been proved to be effective in controlling the vortex of a wing [14−18].

With the results of the previous section, it can be concluded that the inner wing of type C can provide the maximum contribution in lift enhancement. So, aerodynamic enhancement for a broad range of angles, such as the lift-to-drag ratio, can be achieved by combining the inner wing control of type C and the outer wing control of type A.

4 Discussion

The underlying mechanism of NS-DBD plasma actuation may be that the plasma actuator can enhance boundary layer momentum transport, bringing high momentum fluid into the separated region. Lift enhancement can be obtained only at high angles of attack, which indicates that the plasma actuation can effectively control the separation on the wing's leading edge. The experiment also shows that an improvement in lift enhancement can be obtained at a low actuator frequency. This may be because the frequency is of the same order as the natural shedding of vortices of the wing model, which could be assessed by the reduced frequency F^+. In this experiment, the reduced frequency F^+ is 1.35 and 6.73, corresponding to pulsed frequency 0.2 kHz and 1 kHz. So, strong coupling exists between plasma actuation and free-stream flow. Furthermore,

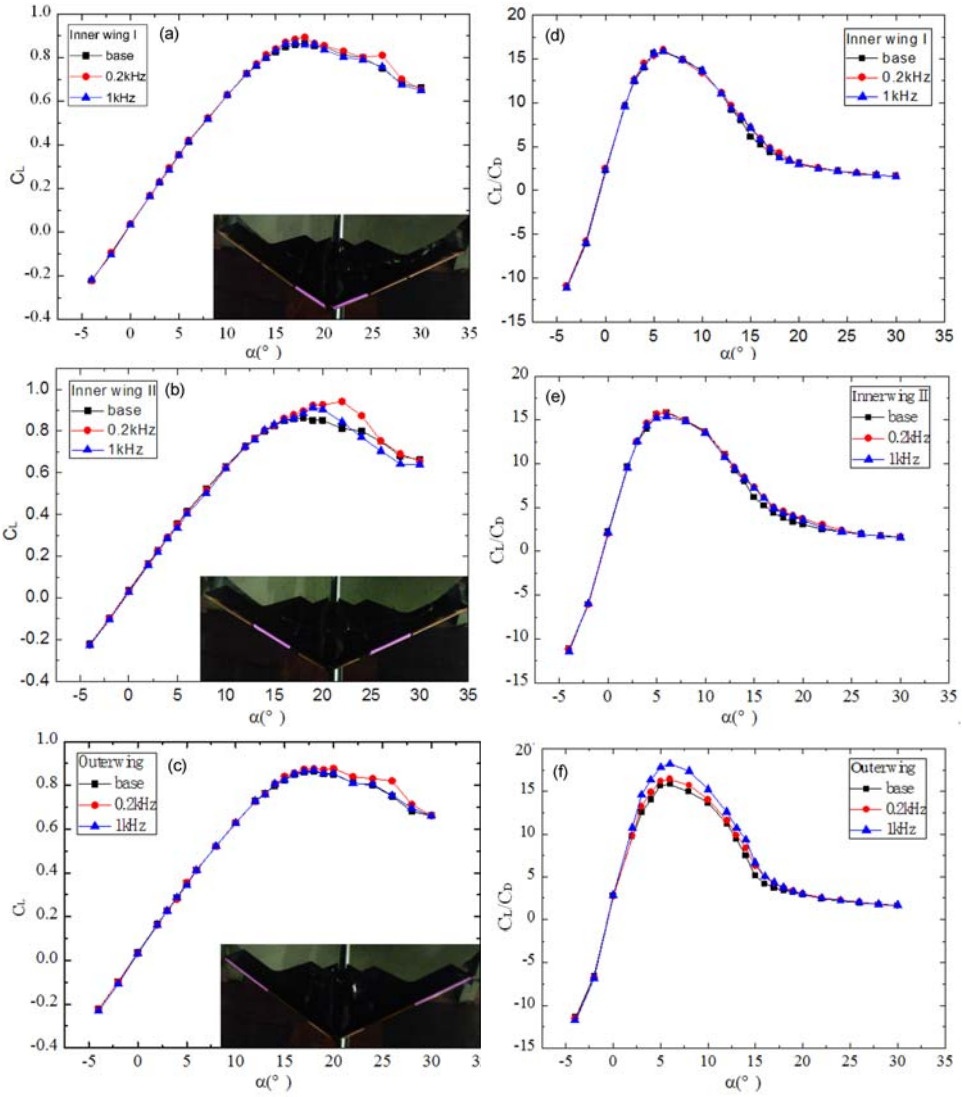

(a) Lift coefficient, inner wing I, (b) Lift coefficient, inner wing II, (c) Lift coefficient, outer wing, (d) Lift-to-drag ration, inner wing I, (e) Lift-to-drag ratio, inner wing II, (f) Lift-to-drag ration, outer wing

Fig.10 Results of distributed plasma actuation

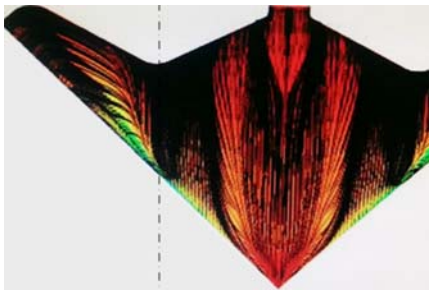

Fig.11 Oil flow at 10° of 1303 UAV [19]

the effectiveness in separation control is improved when a plasma actuator is fixed at the type C location on inner wing II, where leading edge separation occurs along the wing's leading edge. This may be because the perturbation generated by the plasma actuator can be amplified and delivered by the strong shear layer on the leading edge. However, the effectiveness in drag reduction is enhanced when the plasma actuator is fixed at the type A location on the outer wing at a pulsed frequency of f=1 kHz. This may be because the leading edge vortex is the main feature for a swept wing, which can be generated on the wing tip even at low angles of attack. So, high frequency actuation may cause an obvious change on the vortex, which results in a decrease in the drag coefficient. Fig. 12 shows a probable schematic diagram of the main mechanism of aerodynamic control on the flying wing.

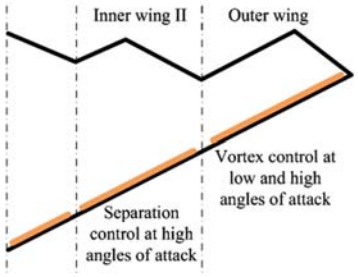

Fig.12 The probable schematic diagram of the main mechanism

5 Conclusion

A new application of leading edge NS-DBD plasma actuation to aerodynamic control on a flying-wing-type model with a 35° swept angle was investigated at subsonic flow speed with the Reynolds number 4.6×10^5. Some important conclusions are drawn as follows.

The results indicate that the NS-DBD plasma actuator offers tremendous potential to enhance the aerodynamic performance of the present model. The test also indicates that control efficiency demonstrates strong dependence on actuator frequency and location. Synchronously, slight enhancement in the static stability in the longitudinal channel can also be achieved with plasma actuation.

An obvious improvement in the lift coefficient is obtained for type C plasma actuators at a pulsed frequency of f=0.2 kHz. This indicates that plasma actuation can be useful for flight control at high angles of attack where conventional flaps may be ineffective under other conditions such as landing. Given the high pulsed frequency of f=1 kHz, an obvious decrease in the drag coefficient is observed for type A plasma actuation, resulting in a 22.4% increase in the lift-to-drag ratio at a low angle of attack, indicating that plasma actuation can enhance the take-off and climbing performance of the flying wing at low angles of attack and low flow speed.

With plasma actuation in a distributed manner, two important conclusions are acquired. Plasma actuation at different positions of the leading edge results in an obvious distinguishable improvement in aerodynamic control. Control at the inner wing plays an important role in lift enhancement, whereas control at the outer wing can reduce drag at low angles of attack, which is the result of vortex control by plasma actuation. From a practical point of view, a combination of distributed plasma actuators may achieve greater improvement in aerodynamic performance.

References

1 Dmitriev Vladimir G, Shkadov Leonid M, Denisov Vladimir E, et al. 2003. The Flying-wing Concept-Chances and Risks. AIAA Paper 2003-2887

2 Huber Kerstin C, Schütte Andreas, Rein Martin. 2006. Numerical Investigation of the Aerodynamic Properties of a Flying Wing Configuration. AIAA Paper 2006-3495

3 Melton L Pack, Yao C S, Seifert A. 2006, AIAA Journal, 44: 34

4 Gad-el-Hak Mohamed. 2001, Journal of Aircraft, 38: 402

5 Corke T C, Post M L, Orlov D M. 2008, Journal of Propulsion and Power, 24: 935

6 Grundmann S, Tropea C. 2007, Experiments in Fluids, 42: 653

7 Benard N, Bonnet J P, Touchard G, et al. 2008, AIAA Journal, 46: 2293

8 Post M L, Corke T. 2004, AIAA Journal, 42: 2177

9 Enloe C L, McLaughlin Thomas E, VanDyken Robert D, et al. 2004, AIAA Journal, 42: 595

10 Takashima Keisuke, Zuzeek Yvette, Lempert Walter R, et al. 2010. Characterization of Surface Dielectric Barrier Discharge Plasma Sustained by Repetitive Nanosecond Pulses. AIAA Paper 2010-4764

11 Roupassov D V, Nikipelov A A, Nudnova M M, et al. 2009, AIAA Journal, 47: 168

12 Wu Y, Li Y H, Zhou M, et al. 2009. Plasma Aerodynamic Actuation Based Corner Separation Control in a Compressor Cascade. AIAA Paper 2009-4070

13 Sun Q, Cheng B Q, Li Y H, et al. 2013. Plasma Science and Technology, 15: 1136

14 Greenblatt D, Kastantin Y, Nayeri C N, et al. 2007. Delta Wing Flow Control Using Dielectric Barrier Discharge Actuators. AIAA Paper 2007-4277

15 Greenblatt D, Kastantin Y, Nayeri C N, et al. 2008, AIAA Journal, 46: 1554

16 Maslov Anatoly, Sidorenko Andrey A, Zanin Boris Yu, et al. Plasma Control of Flow Separation on Swept Wing at High Angles of Attack. AIAA Paper 2008-540

17 Budovsky Alexey D, Sidorenko Andrei A, Maslov Anatoly A, et al. 2009. Plasma Control of Vortex Flow on Delta-Wing At High Angles Of Attack. AIAA Paper 2009-888

18 Patel Mehul P, Ng T Terry, Vasudevan Srikanth, et al. 2007, Journal of Aircraft, 44: 1264

19 Nelson Robert C, Corke Thomas C, Othman Hesham, et al. 2008. A Smart Wing Turbine Blade Using Distributed Plasma Actuators for Improved Performance. AIAA Paper 2008-1312

20 Atkinson Michael, Ferguson Frederick. 2006. A Computational Fluid Dynamics Investigation of the 1303 UCAV Configuration with Deployable Rao Vortex Flaps. AIAA Paper 2006-1262

(Manuscript received 25 September 2014)
(Manuscript accepted 1 December 2014)
E-mail address of corresponding author LIANG Hua: lianghua82702@tom.com